Switchable Cyanometalates

Deutsche Ausgabe: DOI: 10.1002/ange.201601526
Internationale Ausgabe: DOI: 10.1002/anie.201601526

Charge-Transfer Phase Transition of a Cyanide-Bridged Fe^{II}/Fe^{III} Coordination Polymer

Kuirun Zhang, Soonchul Kang, Zi-shuo Yao, Kazusa Nakamura, Takashi Yamamoto, Yasuaki Einaga, Nobuaki Azuma, Yuji Miyazaki, Motohiro Nakano, Shinji Kanegawa, and Osamu Sato**

Abstract: *Heterometallic Prussian blue analogues are known to exhibit thermally induced charge transfer, resulting in switching of optical and magnetic properties. However, charge-transfer phase transitions have not been reported for the simplest FeFe cyanide-bridged systems. A mixed-valence Fe^{II}/Fe^{III} cyanide-bridged coordination polymer, $\{[Fe(Tp)(CN)_3]_2Fe(bpe)\cdot 5H_2O\}_n$, which demonstrates a thermally induced charge-transfer phase transition, is described. As a result of the charge transfer during this phase transition, the high-spin state of the whole system does not change to a low-spin state. This result is in contrast to FeCo cyanide-bridged systems that exhibit charge-transfer-induced spin transitions.*

Molecular materials possessing reversible switchable physical properties in the solid state are attracting considerable interest in view of their potential applications as multifunctional molecular devices, including ultrahigh-density data storage technologies and sensors.[1–3] Various switchable compounds were recently reported, such as spin-crossover complexes,[4–6] valence tautomeric compounds,[7,8] and heterobimetallic and/or multinuclear mixed-valence compounds, where thermally induced charge transfers occur between the two redox-active metal ions.[9–11]

The most prevalent compounds exhibiting reversible charge-transfer phase transitions are Prussian blue analogues: FeCo,[12–16] FeMn,[17,18] FeW,[19] FeOs,[20] CoW,[21,22] CoOs,[23] MoCu,[24] and FeCoW[25] cyanide-bridged systems. Some of these compounds demonstrate coupled charge transfers and spin transitions (charge-transfer-induced spin transitions; CTISTs), yielding molecular photomagnets, humidity sensors, and molecular actuators.[26–28] However, switchable magnetic properties resulting from thermally induced metal-to-metal charge transfers (MMCTs) through cyanide bridges have not been reported for the simplest FeFe cyanide-bridged systems. The prototypical compound, Prussian blue ($Fe^{III}_4[Fe^{II}(CN)_6]_3\cdot x H_2O$), does not exhibit MMCT phase transitions; its electrochemical and/or chemical switching has only been demonstrated in Prussian white (Everitt's salt; Fe^{II}-CN-Fe^{II} units) and Prussian brown (Fe^{III}-CN-Fe^{III} units) through a $Fe^{3+/2+}$ redox reaction in the solid state.[29,30] In a continuing effort to obtain switchable cyanometalates, cyanide-bridged iron complexes with either Fe^{III}-CN-Fe^{II} or Fe^{II}-CN-Fe^{III} units have been reported.[31–36] Therefore, appropriate control of the redox potential of iron ions in these complexes might allow for the transformation of Fe^{III}-CN-Fe^{II} into Fe^{II}-CN-Fe^{III} through a MMCT phase transition in the simplest FeFe Prussian blue analogues.

Herein, we present a cyanide-bridged iron complex exhibiting thermally induced charge transfers between Fe^{II} and Fe^{III} metal ions, resulting in significant changes in magnetic and optical properties. A coordination polymer, $\{[Fe(Tp)(CN)_3]_2Fe(bpe)\cdot 5H_2O\}_n$ (**1**; Tp = hydrotris(pyrazolyl)borate; bpe = 1,2-bis(4-pyridyl)ethane), shows a reversible temperature-induced charge transfer, where the high-temperature (HT) phase has an $Fe^{III\text{-}LS}$-CN-$Fe^{II\text{-}HS}$-NC-$Fe^{III\text{-}LS}$ (HS = high-spin, LS = low-spin) electronic structure, while the low-temperature (LT) phase has an $Fe^{II\text{-}LS}$-CN-$Fe^{III\text{-}HS}$-NC-$Fe^{III\text{-}LS}$ electronic structure. In the LT phase, compound **1** possesses an electronic state similar to that of both Prussian blue ($Fe^{II\text{-}LS}$-CN-$Fe^{III\text{-}HS}$) and Prussian brown ($Fe^{III\text{-}LS}$-CN-Fe^{III}). Notably, the homeotypical FeCo system[37] ($\{[Fe(Tp)(CN)_3]_2$-$Co(bpe)\cdot 5H_2O\}_n$), exhibits CTIST from an HT phase ($Fe^{III\text{-}LS}$-CN-$Co^{II\text{-}HS}$-NC-$Fe^{III\text{-}LS}$) into an LT phase ($Fe^{II\text{-}LS}$-CN-$Co^{III\text{-}LS}$-NC-$Fe^{III\text{-}LS}$). By comparison, **1** displays a thermally induced MMCT phase transition without spin transition.

The target compound was synthesized by reaction of $(Bu_4N)[Fe(Tp)(CN)_3]$ with $Fe(ClO_4)_2\cdot 6H_2O$ and bpe in a 2:1:1 molar ratio in MeOH. Single-crystal X-ray studies at 240 K revealed that **1** crystallizes as the monoclinic space group $P2_1/n$. Additionally, the asymmetric unit of **1** consists of two unique Fe^{III} centers and one unique Fe^{II} center, yielding neutral, mixed-valence, $[Fe^{III}(Tp)(CN)_3]_2Fe^{II}(bpe)$ coordination polymer layers with intercalated, uncoordinated water molecules. Within the neutral unit, the $[Fe^{III}(Tp)(CN)_3]^-$ anion engages in multiple coordinative interactions, forming a bridge between two Fe^{II} ions with two of its *cis*-positioned cyanide groups. Each Fe^{II} center coordinates to four nitrogen atoms from the CN^- bridges, affording mixed-valence $Fe^{III}_2Fe^{II}$ double-zigzag chains running parallel to the *a* axis

[*] Dr. K. Zhang, Dr. S. Kang, Dr. Z. Yao, K. Nakamura, Dr. S. Kanegawa, Prof. Dr. O. Sato
Institute for Materials Chemistry and Engineering, Kyushu University
744 Motooka Nishi-ku Fukuoka, 819-0395 (Japan)
E-mail: kang@cm.kyushu-u.ac.jp
sato@cm.kyushu-u.ac.jp
Dr. T. Yamamoto, Prof. Dr. Y. Einaga
Department of Chemistry, Keio University
3-14-1 Hiyoshi, Yokohama 223-8522 (Japan)
N. Azuma, Dr. Y. Miyazaki, Prof. Dr. M. Nakano
Research Center for Structural Thermodynamics, Graduate School of Science, Osaka University
Toyonaka, Osaka 560-0043 (Japan)

Supporting information for this article can be found under: http://dx.doi.org/10.1002/anie.201601526.

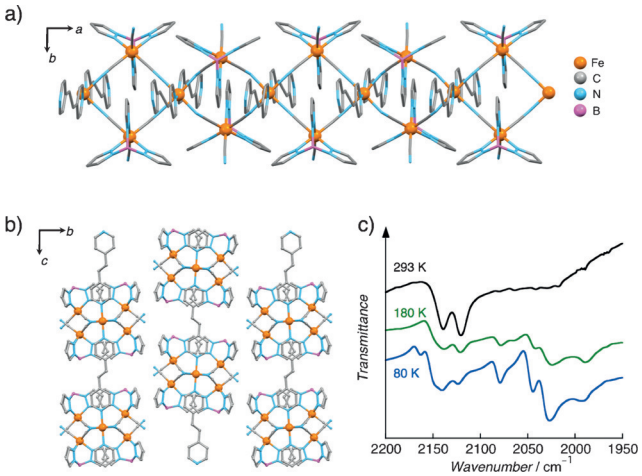

Figure 1. a) Crystal structure of $\{[Fe(Tp)(CN)_3]_2Fe(bpe)\cdot 5H_2O\}_n$ (**1**) coordination polymer along the *c* axis. Fe: orange, N: blue, C: gray, and B: pink. b) Packing structure of **1** along the *a* axis. c) Variable-temperature solid-state infrared spectra of **1**.

(Figure 1a). The chain structure was similar to that of previously reported bimetallic double-zigzag chains. The chains are further linked by bpe ligands along the apical positions of the Fe^{II} centers, affording a framework structure (Figure 1b). Each Fe^{II} center is located in an octahedral environment framed by six nitrogen donors: four short equatorial Fe–N distances (2.121(7)–2.153(7) Å) and two longer apical Fe–N distances (2.207(6)–2.214(6) Å). The average Fe^{III}–C and Fe^{III}–N bond distances of two $[Fe^{III}(Tp)(CN)_3]^-$ units are about 1.903 and 1.981 Å, respectively (Supporting Information, Table S1). Bond valence sum and charge compensation indicates that at 240 K the Fe^{II} center is in a HS state, while the Fe^{III} center is in a LS state, forming the electronic structure with $Fe^{III\text{-}LS}$-CN-$Fe^{II\text{-}HS}$-NC-$Fe^{III\text{-}LS}$.

Upon cooling of the crystal to 123 K, the space group of **1** did not change. However, the Fe–N distances of the iron ion in the N6 octahedral environment shorten to an average distances of 2.077 Å, which is a decrease of about 0.086 Å compared to that observed at 240 K (2.163 Å). Most Fe^{II} ions in the N6 octahedral environment show spin transition upon decrease of the Fe–N bond distances by approximately 0.2 Å. Therefore, the decrease seen in **1** is smaller than that expected for the spin transition from $Fe^{II\text{-}HS}$ to $Fe^{II\text{-}LS}$. However, the Fe^{III}-N distances are generally smaller than those of Fe^{II}-N. Thus, we can assume that charge transfer is possible between metal ions upon cooling, yielding an $Fe^{II\text{-}LS}$-CN-$Fe^{III\text{-}HS}$-NC-$Fe^{III\text{-}LS}$ electronic structure. This assumption was supported by variable-temperature IR spectroscopy. Namely, the IR spectrum of **1** at 293 K contains two cyano stretching absorptions (ν_{CN}), corresponding to the free ν_{CN} absorption (2120 cm^{-1}) of the $[Fe^{III}(Tp)(CN)_3]^-$ unit and the bridging ν_{CN} absorption (2140 cm^{-1}) of $Fe^{III\text{-}LS}$(μ-CN)$Fe^{II\text{-}HS}$ linkages (Figure 1c). Upon cooling from 293 K to 80 K, new ν_{CN} stretches appear (2078, 2044, and 2026 cm^{-1}), which could be attributed to the presence of $Fe^{II\text{-}LS}$(μ-CN)$Fe^{III\text{-}HS}$ linkages. Furthermore, the initial spectrum was recovered upon heating.

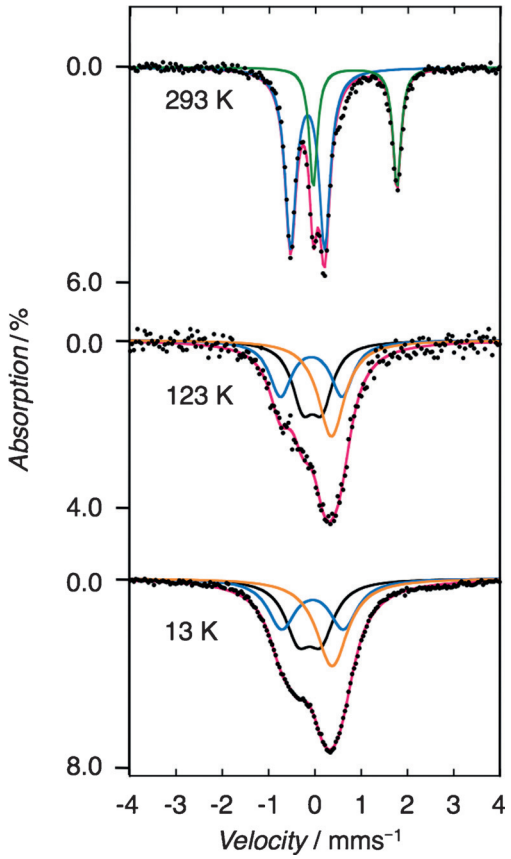

Figure 2. Mössbauer spectra of **1** obtained at various temperatures.

The ^{57}Fe Mössbauer spectrum of **1** was measured at 293, 123, and 13 K (Figure 2). At 293 K, the spectrum is composed of two quadrupole doublets with Mössbauer parameters characteristic of HS Fe^{II} and LS Fe^{III} ions ($\delta = 0.949$ and $\Delta E_Q = 1.426$ mm s^{-1}, and $\delta = -0.160$ and $\Delta E_Q = 0.801$ mm s^{-1}, respectively). The peak area ratio of the two doublets is $Fe^{II}/Fe^{III} = 0.35/0.65$, which is consistent with the oxidation states estimated from the structural data of the HT phase. However, upon cooling to 13 K, the $Fe^{II\text{-}HS}$ absorption disappears completely and a new doublet and singlet appear corresponding to the $Fe^{III\text{-}HS}$ and $Fe^{II\text{-}LS}$, respectively. The peak intensity ratio of $Fe^{III\text{-}LS}/Fe^{III\text{-}HS}/Fe^{II\text{-}LS} = 0.32/0.34/0.34$ indicates that a thermally induced charge transfer occurs between the iron centers, which can be expressed as an interchange of $Fe^{III\text{-}LS}$-CN-$Fe^{II\text{-}HS}$-NC-$Fe^{III\text{-}LS}$ (HT phase) and $Fe^{II\text{-}LS}$-CN-$Fe^{III\text{-}HS}$-NC-$Fe^{III\text{-}LS}$ (LT phase). As mentioned above, during this charge-transfer phase transition, the Fe^{HS} sites do not experience spin-state conversion, which is in sharp contrast with the FeCo system: $\{[Fe(Tp)(CN)_3]_2Co(bpe)\cdot 5H_2O\}_n$ exhibits thermally induced CTIST.[37]

Figure 3 shows the temperature dependence of the $\chi_m T$ values of **1**. Between 270 and 245 K, the $\chi_m T$ value remains nearly constant at 6.0 $cm^3 mol^{-1} K$, corresponding to the presence of one $Fe^{II\text{-}HS}$ and two $Fe^{III\text{-}LS}$ with significant orbital contributions. Upon cooling, the $\chi_m T$ values decrease at approximately 200–245 K, reaching a minimum value of 5.4 $cm^3 mol^{-1} K$ at 150 K. The cooling–heating mode measurement reveals the presence of a reversible signal without

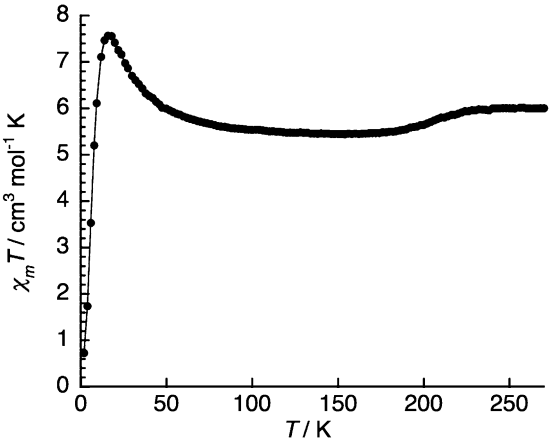

Figure 3. Temperature dependence of the $\chi_m T$ values of **1** (applied magnetic field: 5000 Oe). A solid line is provided to aid the eye.

thermal hysteresis. This magnetic feature confirms the occurrence of a reversible charge-transfer process involving the reversible transformation of $Fe^{III\text{-}LS}$-CN-$Fe^{II\text{-}HS}$-NC-$Fe^{III\text{-}LS}$ (HT phase) into $Fe^{II\text{-}LS}$-CN-$Fe^{III\text{-}HS}$-NC-$Fe^{III\text{-}LS}$ (LT phase). The $\chi_m T$ values then increase with decreasing temperature, reaching a maximum value of 7.6 $cm^3 mol^{-1} K$ at 16 K, suggesting the presence of ferromagnetic interactions between iron ions. As the temperature further decreased to 2 K, the $\chi_m T$ values abruptly decreased because of interchain antiferromagnetic interactions. A more detailed description of magnetic curves in the LT phase is included in the Supporting Information, Figure S2.

To elucidate the driving force of the charge-transfer phase transition, the heat capacity of **1** was measured between 7 and 300 K by adiabatic calorimetry (Figure 4), revealing two anomalies. The first is a small peak at 142 K with a transition entropy of 4.29 $J K^{-1} mol^{-1}$, which most likely arises from an order–disorder transition (ca. $R\ln(2) = 5.76\ J K^{-1} mol^{-1}$, where R is the gas constant). The second is a broad heat capacity anomaly centered at 237 K, which most likely corresponds to an electron-transfer phenomenon, as the transition temperature is consistent with the temperature at which the anomaly was observed by magnetic susceptibility measurements. The excess heat capacity (ΔC_p) was then determined by subtracting the normal portion from the experimental data (Figure 4b). Integration of the excess heat capacity yields the enthalpy and entropy that arose from the charge-transfer phenomenon, which are approximately 4.51 $kJ mol^{-1}$ and 19.25 $J K^{-1} mol^{-1}$, respectively. Note that the transition entropy obtained here is much greater than the spin-only value expected for the change in the spin multiplicity between the HT ($Fe^{III\text{-}LS}$-CN-$Fe^{II\text{-}HS}$) and LT ($Fe^{II\text{-}LS}$-CN-$Fe^{III\text{-}HS}$) phases, which is approximately $R\ln(10/6) = 4.25\ J K^{-1} mol^{-1}$. This excess contribution over spin entropy (ca. 15 $J K^{-1} mol^{-1}$) is attributed to the frequency shifts of molecular and lattice vibrations upon MMCT phase transition, rather than the change of electronic degeneracy of d-electrons, because the lower-symmetry ligand field in **1** lifts the orbital degeneracy of T-term iron ions in the HT phase, providing a non-degenerate ground state. The presence of vibrational entropy is also consistent with the temperature dependence of CN stretching modes noted earlier, although the amount is not as large as in conventional spin-crossover transitions.[38] As a result of the difference in single-center electron transfer (spin-crossover) remarkable softening of breathing mode and two-center MMCT arises, where softening in one center is well-compensated with hardening of another center. This situation is also reported for a similar MMCT systems, $(n\text{-}C_3H_7)_4N[Fe^{II}Fe^{III}(dto)_3]$ (dto = 1,2-dithiooxalate).[39]

To clarify the nature of the mixed-valence state of **1**, UV/Vis-NIR absorption spectra for **1** were measured in the 350–2500 nm range. According to the Robin and Day classification,[40,41] the half-bandwidth ($\Delta\bar{\nu}_{1/2}$) at the optical intervalence charge-transfer (IVCT) transition has been used as a criterion for distinguishing between Class II and III transitions and is calculated using Equation (1):

$$\Delta\bar{\nu}_{1/2} = [2312\bar{\nu}_{max}]^{1/2}\ (cm^{-1}, \text{at } 300\ K), \quad (1)$$

where $\bar{\nu}_{max}$ is the intervalence band maximum. At 300 K, **1** exhibits a broad IVCT band ($\lambda_{max} \approx 1300$ nm, $E_{OP} = 0.95$ eV; see Figure 5), where the bandwidth of the IVCT fits the relationship described by Equation (1) well ($\Delta\bar{\nu}_{1/2}(calcd) = 4219\ cm^{-1}$, $\Delta\bar{\nu}_{1/2}(obsd) = 4217\ cm^{-1}$; Supporting Information, Figure S5), indicating a Class II system. Futhermore, compound **1** shows thermochromic behavior in the NIR region. On cooling to 80 K, new high-energy, intense absorption occurs around 1130 nm ($E_{OP} = 1.1$ eV).

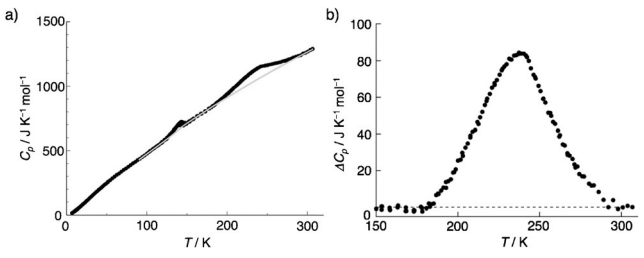

Figure 4. a) Temperature dependence of the molar heat capacity of **1**. The gray curve shows the normal heat capacity. b) Excess molar heat capacity (ΔC_p) arising from the charge-transfer phase transition of **1**.

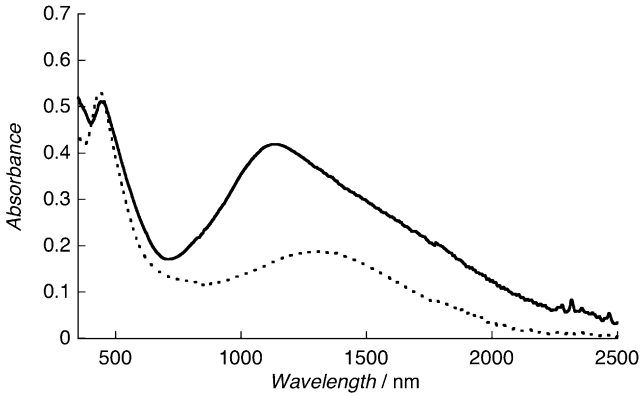

Figure 5. UV/Vis-NIR absorption spectra of **1** at 80 K (solid line) and 300 K (dotted line).

In conclusion, the mixed-valence Fe^{II}/Fe^{III} coordination polymer described herein demonstrates a temperature-induced MMCT phase transition. To date, a number of Prussian blue analogues exhibiting MMCT between hetero-metals have been reported. To our knowledge, compound **1** is the first example of a homometallic cyanide-bridged system exhibiting thermally induced MMCT phase transitions. In contrast to FeCo systems, the charge transfer in compound **1** is not coupled to spin transition. Furthermore, compound **1** in the LT phase contains both Prussian blue ($Fe^{II\text{-}LS}$-CN-$Fe^{III\text{-}HS}$) and Prussian brown ($Fe^{III\text{-}LS}$-CN-Fe^{III}) type electronic states, yielding strong absorption in the visible and near-infrared regions. As such, this study encourages the rational design of dynamic molecules that exhibit dynamic changes in their properties in response to external stimuli.

Acknowledgements

This work was supported by a JSPS KAKENHI Grant, numbers 26810039, 25288029, and 15H01018. This work was partly supported by Nanotechnology Platform Program (Molecule and Material Synthesis) of the Ministry of Education, Culture, Sports, Science and Technology (MEXT), Japan. A part of this work was performed at the BL02B1 of SPring-8 with the approval of the Japan Synchrotron Radiation Research Institute (JASRI; Proposal No. 2014B1471).

Keywords: charge transfer · cyanide complexes · iron · mixed-valence · phase transitions

How to cite: *Angew. Chem. Int. Ed.* **2016**, *55*, 6047 – 6050
Angew. Chem. **2016**, *128*, 6151 – 6154

[1] C. Joachim, J. K. Gimzewski, A. Aviram, *Nature* **2000**, *408*, 541.
[2] O. Kahn, C. J. Martinez, *Science* **1998**, *279*, 44.
[3] V. Balzani, A. Credi, *Chem. Rec.* **2001**, *1*, 422.
[4] A. Bousseksou, G. Molnár, L. Salmon, W. Nicolazzi, *Chem. Soc. Rev.* **2011**, *40*, 3313.
[5] M. A. Halcrow, *Spin-crossover materials: properties and applications*, Wiley, Oxford, **2013**.
[6] T. Matsumoto, G. N. Newton, T. Shiga, S. Hayami, Y. Matsui, H. Okamoto, R. Kumai, Y. Murakami, H. Oshio, *Nat. Commun.* **2014**, *5*, 3865.
[7] V. I. Minkin, A. A. Starikova, *Mendeleev Commun.* **2015**, *25*, 83.
[8] O. Sato, A. Cui, R. Matsuda, J. Tao, S. Hayami, *Acc. Chem. Res.* **2007**, *40*, 361.
[9] O. N. Risset, P. A. Quintero, T. V. Brinzari, M. J. Andrus, M. W. Lufaso, M. W. Meisel, D. R. Talham, *J. Am. Chem. Soc.* **2014**, *136*, 15660.
[10] Y. Zhang, D. Li, R. Clérac, M. Kalisz, C. Mathonière, S. M. Holmes, *Angew. Chem. Int. Ed.* **2010**, *49*, 3752; *Angew. Chem.* **2010**, *122*, 3840.
[11] A. Bleuzen, V. Marvaud, C. Mathoniere, B. Sieklucka, M. Verdaguer, *Inorg. Chem.* **2009**, *48*, 3453.
[12] C. P. Berlinguette, A. Dragulescu-Andrasi, A. Sieber, H. U. Güdel, C. Achim, K. R. Dunbar, *J. Am. Chem. Soc.* **2005**, *127*, 6766.
[13] M. Nihei, Y. Sekine, N. Suganami, K. Nakazawa, A. Nakao, H. Nakao, Y. Murakami, H. Oshio, *J. Am. Chem. Soc.* **2011**, *133*, 3592.
[14] T. Liu, D.-P. Dong, S. Kanegawa, S. Kang, O. Sato, Y. Shiota, K. Yoshizawa, S. Hayami, S. Wu, C. He, C.-Y. Duan, *Angew. Chem. Int. Ed.* **2012**, *51*, 4367; *Angew. Chem.* **2012**, *124*, 4443.
[15] N. Hoshino, F. Iijima, G. N. Newton, N. Yoshida, T. Shiga, H. Nojiri, A. Nakao, R. Kumai, Y. Murakami, H. Oshio, *Nat. Chem.* **2012**, *4*, 921.
[16] E. S. Koumousi et al., *J. Am. Chem. Soc.* **2014**, *136*, 15461.
[17] H. Tokoro, S. Ohkoshi, T. Matsuda, K. Hashimoto, *Inorg. Chem.* **2004**, *43*, 5231.
[18] H. Tokoro, S. Ohkoshi, *Bull. Chem. Soc. Jpn.* **2015**, *88*, 227.
[19] S. Chorazy et al., *Chem. Commun.* **2014**, *50*, 3484.
[20] M. G. Hilfiger, M. Chen, T. V. Brinzari, T. M. Nocera, M. Shatruk, D. T. Petasis, J. L. Musfeldt, C. Achim, K. R. Dunbar, *Angew. Chem. Int. Ed.* **2010**, *49*, 1410; *Angew. Chem.* **2010**, *122*, 1452.
[21] S. Ohkoshi, S. Ikeda, T. Hozumi, T. Kashiwagi, K. Hashimoto, *J. Am. Chem. Soc.* **2006**, *128*, 5320.
[22] R. Le Bris, Y. Tsunobuchi, C. Mathonière, H. Tokoro, S. Ohkoshi, N. Ould-Moussa, G. Molnar, A. Bousseksou, J. F. Létard, *Inorg. Chem.* **2012**, *51*, 2852.
[23] C. Avendano, M. G. Hilfiger, A. Prosvirin, C. Sanders, D. Stepien, K. R. Dunbar, *J. Am. Chem. Soc.* **2010**, *132*, 13123.
[24] J. M. Herrera, V. Marvaud, M. Verdaguer, J. Marrot, M. Kalisz, C. Mathoniere, *Angew. Chem. Int. Ed.* **2004**, *43*, 5468; *Angew. Chem.* **2004**, *116*, 5584.
[25] R. Podgajny, S. Chorazy, W. Nitek, M. Rams, A. M. Majcher, B. Marszalek, J. Zukrowski, C. Kapusta, B. Sieklucka, *Angew. Chem. Int. Ed.* **2013**, *52*, 896; *Angew. Chem.* **2013**, *125*, 930.
[26] O. Sato, J. Tao, Y. Z. Zhang, *Angew. Chem. Int. Ed.* **2007**, *46*, 2152; *Angew. Chem.* **2007**, *119*, 2200.
[27] H. J. Shepherd, I. A. Gural'skiy, C. M. Quintero, S. Tricard, L. Salmon, G. Molnar, A. Bousseksou, *Nat. Commun.* **2013**, *4*, 2607.
[28] D. M. Pajerowski, J. E. Gardner, D. R. Talham, M. W. Meisel, *J. Am. Chem. Soc.* **2009**, *131*, 12927.
[29] K. Itaya, I. Uchida, V. D. Neff, *Acc. Chem. Res.* **1986**, *19*, 162.
[30] K. Itaya, I. Uchida, *Inorg. Chem.* **1986**, *25*, 389.
[31] M. Shatruk, A. Dragulescu-Andrasi, K. E. Chambers, S. A. Stoian, E. L. Bominaar, C. Achim, K. R. Dunbar, *J. Am. Chem. Soc.* **2007**, *129*, 6104.
[32] M. Nihei, M. Ui, N. Hoshino, H. Oshio, *Inorg. Chem.* **2008**, *47*, 6106.
[33] A. Mondal, Y. Li, P. Herson, M. Seuleiman, M. L. Boillot, E. Rivière, M. Julve, L. Rechignat, A. Bousseksou, R. Lescouëzec, *Chem. Commun.* **2012**, *48*, 5653.
[34] Y.-J. Zhang, T. Liu, S. Kanegawa, O. Sato, *J. Am. Chem. Soc.* **2009**, *131*, 7942.
[35] S. Klokishner, S. Ostrovsky, A. Palii, M. Shatruk, K. Funck, K. R. Dunbar, B. Tsukerblat, *J. Phys. Chem. C* **2011**, *115*, 21666.
[36] S. Kang et al., *Nat. Commun.* **2015**, *6*, 5955.
[37] T. Liu, Y. J. Zhang, S. Kanegawa, O. Sato, *Angew. Chem. Int. Ed.* **2010**, *49*, 8645; *Angew. Chem.* **2010**, *122*, 8827.
[38] M. Sorai, M. Nakano, Y. Miyazaki, *Chem. Rev.* **2006**, *106*, 976.
[39] T. Nakamoto, Y. Miyazaki, M. Itoi, Y. Ono, N. Kojima, M. Sorai, *Angew. Chem. Int. Ed.* **2001**, *40*, 4716; *Angew. Chem.* **2001**, *113*, 4852.
[40] N. S. Hush, *Prog. Inorg. Chem.* **1967**, *8*, 391.
[41] J. P. Launay, M. Verdaguer, *Electrons in Molecules: From Basic Principles to Molecular Electronics*, Oxford University Press, Oxford, **2014**.

Received: February 12, 2016
Published online: April 8, 2016

